Appendix A

Understanding PCC Agent Binding to Single Point Mutation E17K of Akt1 Pleckstrin Homology Domain through Molecular Dynamics

A.1 INTRODUCTION

The Akt kinase is a critical molecular router that mediates cell growth, apoptosis, and translation [1], and Akt overexpression and/or hyperactivation has been observed in many cancer types [2]. The Akt1 activation mechanism includes binding to the PIP3 lipid on the cell membrane with a domain called the Pleckstrin Homology Domain (PHD). Mutations in the PHD of Akt1 that increase its affinity for binding with PIP3 will cause the upregulation of downstream pathways, thereby promoting the formation of cancerous cells [3].

Recent experiments performed on mice have revealed that a single amino acid point mutation to the PHD of Akt1, called the E17K mutation, was sufficient to cause cancer [4]. This same mutation has been found in certain human ovarian, colorectal and breast cancers. The E17K mutation exchanges a negatively charged glutamate for a positively charged lysine, causing the formation of an additional hydrogen bond between the PHD and PIP3 on the cell membrane. This induces a conformational change that causes Akt1(E17K) to bind to the plasma membrane four times stronger than it would in its wild-type form [4]. This strengthened binding is believed to be the underlying mechanism for the creation of a type of cancerous cells in mice.

It is hypothesized that blocking the binding between PIP3 and Akt1(E17K) could reduce or terminate the growth of cancerous cells derived from the E17K mutation in humans, thus serving as a less invasive and less toxic means of chemotherapy. Previous work has shown that peptide capture agents can be raised against Akt that are epitope targeted and/or inhibitory [5,6,7]. Specifically, a 5mer peptide capture agent (yleaf) has

been developed to bind to the E17K mutation of the PH domain of Akt1 [7]. Molecular dynamics (MD) trajectories of the peptide/protein complex are constructed for the anchor with both the mutant and wild type (WT) Akt1 PH domains, and used to calculate the free energy of binding for each system.

A.2 PEPTIDE CAPTURE AGENT AGAINST E17K MUTATION OF AKT1 PHD

Work in the Heath group has yielded a 5mer anchor peptide that differentiates the E17K mutated Akt1 PHD from the wild type domain [7]. The epitope targeted one-bead-one-compound screening method used to identify the ligand provides an anchor point for the C-terminus location of peptide binding. Additionally, biotin labeling experiments done using a variant of the peptide with an N-terminal tosyl-biotin labeling arm indicate a general region of N-terminal peptide interaction with the target around the residue Y26 [8]. These data were used in choosing the initial configuration of the yleaf-tosyl-biotin ligand in relation to either the E17K or WT target.

A.3 CONSTRUCTION OF E17K AND WT SYSTEMS

A.3.1 yleaf-tosyl-biotin

The N-terminal tosyl-biotin labeling arm was constructed in ChemDraw, then imported into Maestro. The bond lengths were manually doubled, and then the B3LYP/6-31G** optimized structure and Mulliken charges were obtained using Jaguar. Unknown bond length, bond angle, and torsion parameters for the tosyl group were

optimized using B3LYP/6-31G** in Jaguar. The yleaf peptide was grown onto the minimized tosyl structure using (D) amino acids to form the complete ligand. yleaf-tosyl-biotin was equilibrated in explicit water at 300 K for 1 ns to obtain the ligand conformation (Figure A.1) used to construct the ligand/protein complexes.

A.3.2 Ligand/Protein Complexes

Crystal structures for E17K (2UZR) and wild type (1UNP) Akt1 PH domains were obtained from the Protein Data Bank. ZDOCK was used to determine an initial relative configuration of the ligand shown in Figure A.1 to the E17K PHD. The anchor peptide was initially screened against the 32mer fragment corresponding to residues 1-32 of the E17K PHD, and ZDOCK predictions were restricted to only include relative conformations that allowed for interaction of the ligand with this fragment. The selected ligand configuration was also used for the wild type PH domain. Figure A.2 shows the top three ZDOCK output structures, and Figure A.3 shows the chosen structure for both E17K and WT systems.

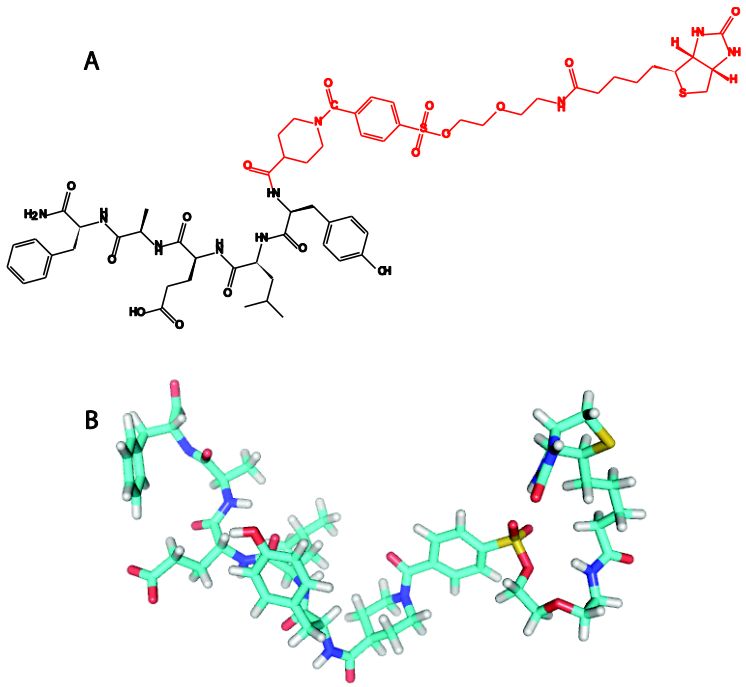

Figure A.1. A. ChemBioDraw structure of yleaf-tosyl-biotin. **B.** Equilibrated structure of yleaf-tosyl-biotin used to construct WT and E17K complexes.

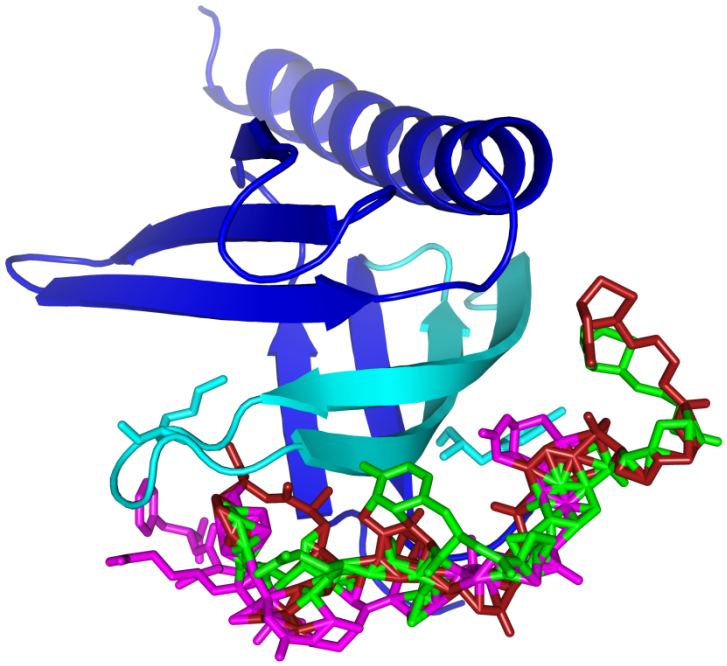

Figure A.2. Top three ZDOCK predicted conformations of yleaf-tosyl-biotin/E17K PH domain complex. Interaction was constrained to occur only with the first 32 residues of the protein (highlighted) that represent the fragment against which the peptide ligand was raised. The two amino acids of interest from experimental binding assays, E17K and Y26, are shown as sticks.

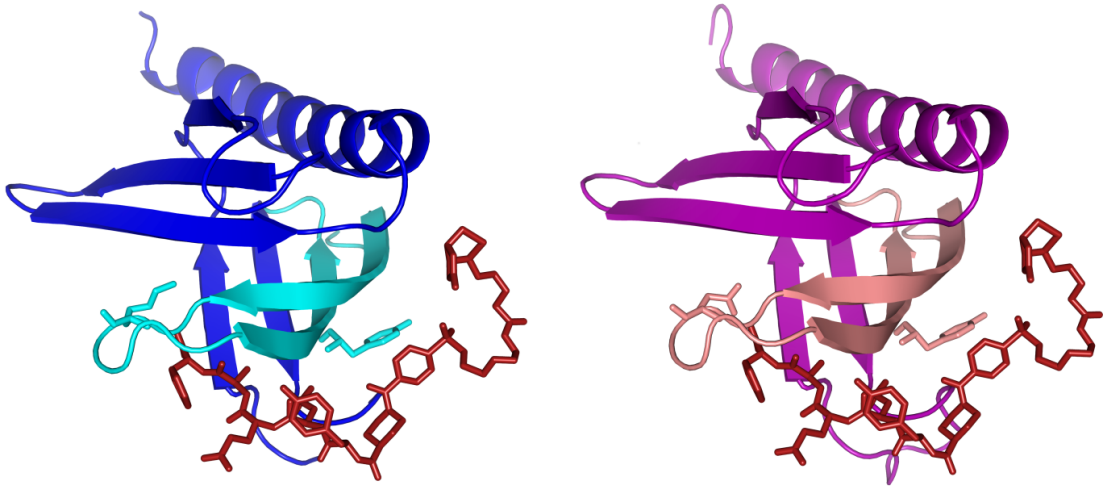

Figure A.3. Selected ligand conformation complexed with the mutant (blue) and wild type (purple) PH domains. This structure was chosen because the ligand most closely spans the two amino acids of interest (E17 or E17K, and Y26).

A.4 MOLECULAR DYNAMICS

The systems were neutralized by adding Cl^- or Na^+ counterions as necessary, and were fully solvated in TIP3P water boxes. Each system was first subjected to a minimization of 10,000 steps. Then the solvent molecules, ligand, and binding fragment were equilibrated for 200 ps at 300 K while the remaining protein coordinates were fixed. The full systems were then minimized for 5,000 steps. Finally, both systems were equilibrated for a total of 5 ns at 300 K. The MD simulations were carried out with the NAMD 2.6 program [9]. Plots of the root mean squared deviation (rmsd) from the initial configuration of the trajectories and restarted trajectories from both systems are shown in Figure A.4.

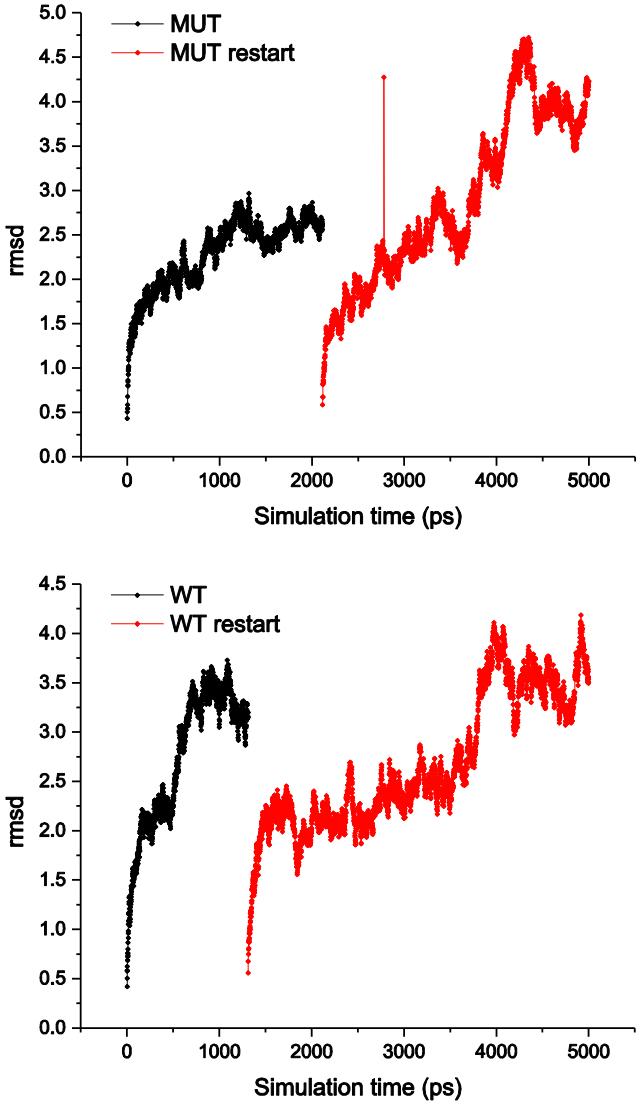

Figure A.4. Rmsd plots for the MD trajectories and restarted trajectories of the E17K and WT complexes.

A.5 BINDING ENERGY

To obtain a good comparison of free binding energy between the two systems, energy landscapes were constructed for E17K and WT by plotting the free energy of binding of conformations representing local macrostates vs. their rmsd from the lowest energy conformation, similar to the approach taken by [10]. If the reference structure is truly the lowest energy, the landscape will be smoothly funnel shaped. If there is an alternative lowest energy structure, the landscape will be non-funnel shaped. Figure A.5 shows examples of this type of landscape, where each dot represents one of 200,000–400,000 independent Rosetta *ab initio* structure prediction simulations [10]. For the purpose of this work, the rmsd of each trajectory is like a partition function, where each point represents a microstate. Plateaus in the rmsd represent macrostates, and given an infinite amount of simulation time, the system will spend a Boltzmann weighted percentage of time in each macrostate. Binding energies were calculated for a number of 100 ps plateaus in each trajectory using a Generalized Born implicit solvent model. After identifying the conformation with the lowest calculated binding energy REF, the energies of the other conformations were plotted against the rmsd of those conformations relative to REF. The energy vs. rmsd plot for the E17K and WT systems are shown in Figures A.6 and A.7, and the structure of the chosen reference structures are shown in Figure A.8. Significantly fewer data points were able to obtained for the E17K and WT systems than the *ab initio* structure prediction simulations, but the plots suggest the funnel shape described by [10], indicating that the correct lowest energy reference structure had been selected.

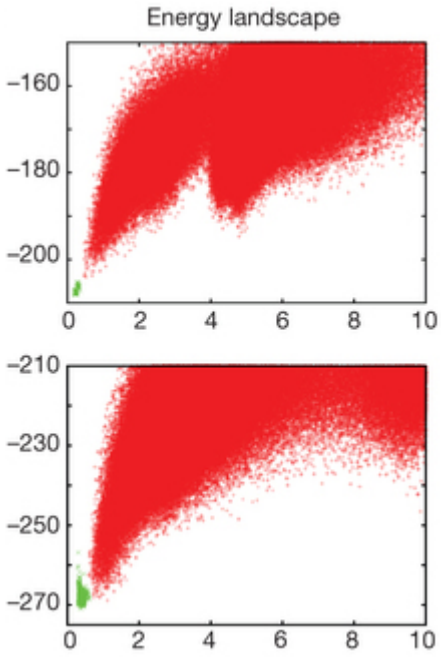

Figure A.5. Energy landscapes obtained from Rosetta *ab initio* structure prediction simulations on Rosetta@home. Red points represent the lowest-energy structures obtained in independent Monte Carlo structure prediction trajectories starting from an extended chain for each sequence; the *y* axis shows the Rosetta all-atom energy and the *x* axis shows the Cα root mean squared deviation from the design model. Green points represent the lowest-energy structures obtained in trajectories starting from the design model. The bottom figure shows a landscape that is funnel shaped, and the top shows one that is non funnel shaped. Adapted from [10].

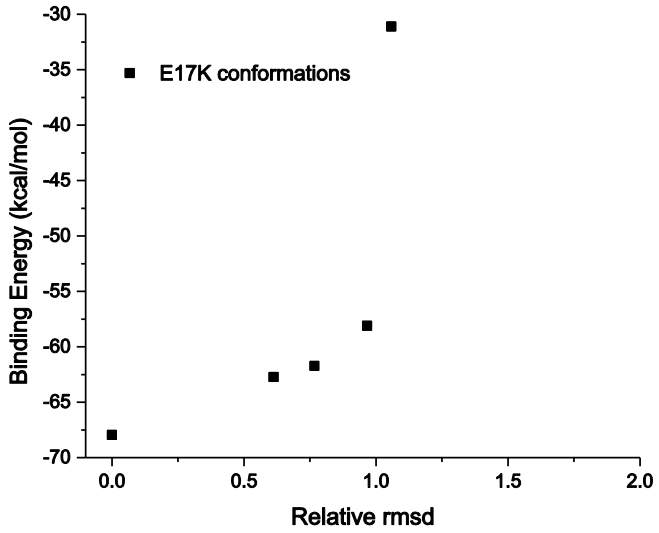

Figure A.6. Energy landscape for E17K complex. The y-axis is the Generalized Born calculation of binding energy, and the x-axis is the rmsd relative to the lowest energy structure. Each point is a plateau in the trajectory rmsd, representing a macrostate of the system. The binding energy of the reference state calculated without including entropy contribution is -67.95 kcal/mol.

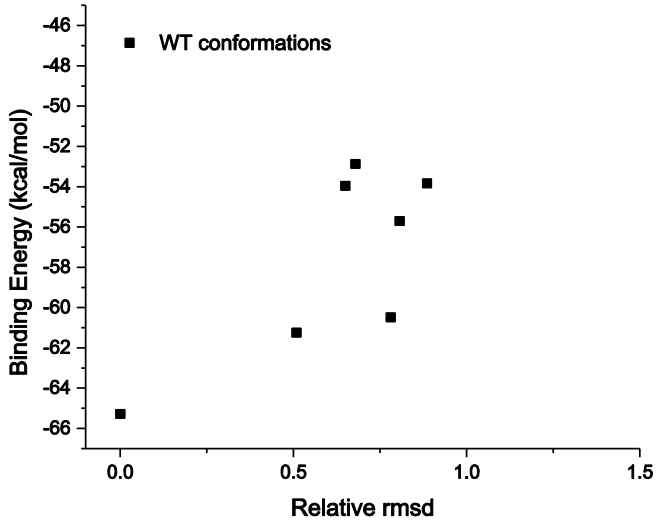

Figure A.7. Energy landscape for WT complex. The y-axis is the Generalized Born calculation of binding energy, and the x-axis is the rmsd relative to the lowest energy structure. Each point is a plateau in the trajectory rmsd, representing a macrostate of the system. The binding energy of the reference state calculated without including entropy contribution is -65.28 kcal/mol.

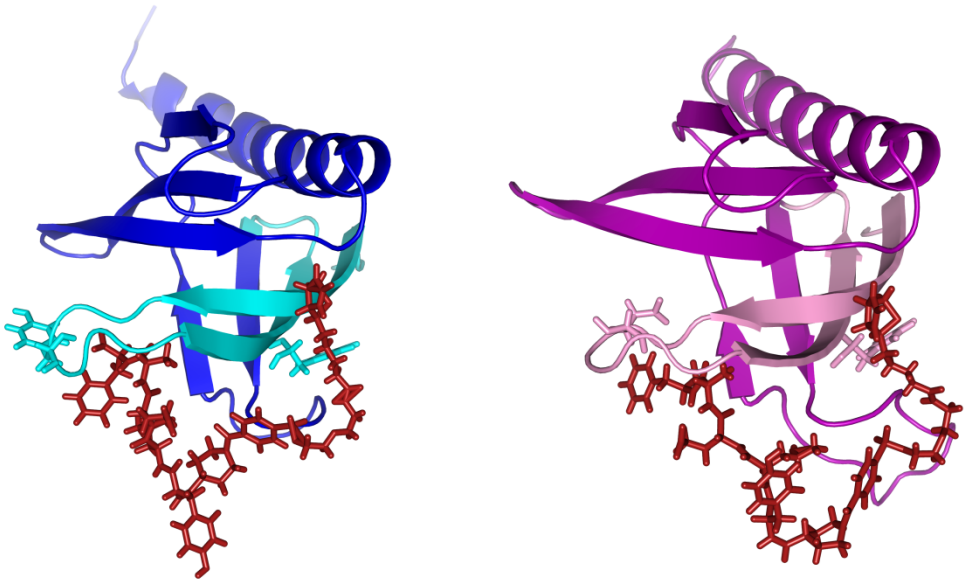

Figure A.8. Structures of the E17K and WT reference states. There are distinct differences in the conformation of the peptide around the E17K mutation cite between the two systems.

A.6 CONCLUSION

This appendix explored the use of MD calculations to understand the selectivity of the peptide ligand yleaf-tosyl-biotin for the E17K mutant of Akt1 PH domain over the wild type domain. The structure of the ligand was constructed and minimized, then complexed with both the E17K and wild type structures of Akt1 PHD. Trajectories were run, and the energies of macrostates of the system were calculated and plotted against their rmsd relative to a reference state to determine if the lowest energy state had been identified. The binding energy of the E17K reference state was found to be 2.67 kcal/mol lower than that of the WT reference state. This corresponds to a factor of ~90 difference in K_d, which is within the error of experimental measurements.

A.7 ACKNOWLEDGEMENTS

This work was done in collaboration with William Goddard III, Kaycie Deyle, and Blake Farrow.

A.8 REFERENCES

1. Vivanco I, Sawyers CL (2002) The phosphatidylinositol 3-kinase–AKT pathway in human cancer. Nature Reviews Cancer 2: 489-501.

2. Altomare DA, Testa JR (2005) Perturbations of the AKT signaling pathway in human cancer. Oncogene 24: 7455-7464.

3. Rebecchi M, Scarlata S (1998) Pleckstrin homology domains: a common fold with diverse functions. Annual review of biophysics and biomolecular structure 27: 503-528.

4. Carpten JD, Faber AL, Horn C, Donoho GP, Briggs SL, et al. (2007) A transforming mutation in the pleckstrin homology domain of AKT1 in cancer. Nature 448: 439-444.

5. Millward SW, Henning RK, Kwong GA, Pitram S, Agnew HD, et al. (2011) Iterative in Situ Click Chemistry Assembles a Branched Capture Agent and Allosteric Inhibitor for Akt1. Journal of the American Chemical Society 133: 18280-18288.

6. Nag A, Das S, Yu MB, Deyle KM, Millward SW, Heath JR (2013) A Chemical Epitope-Targeting Strategy for Protein Capture Agents: The Serine 474 Epitope of the Kinase Akt2. Angewandte Chemie International Edition In press.

7. Deyle K et al., Submitted.

8. Tamura T, Tsukiji S, Hamachi I (2012) Native FKBP12 Engineering by Ligand-Directed Tosyl Chemistry: Labeling Properties and Application to Photo-Cross-Linking of Protein Complexes in Vitro and in Living Cells. Journal of the American Chemical Society 134: 2216-2226.

9. Phillips JC, Braun R, Wang W, Gumbart J, Tajkhorshid E, et al. (2005) Scalable molecular dynamics with NAMD. Journal of computational chemistry 26: 1781-1802.

10. Koga N, Tatsumi-Koga R, Liu G, Xiao R, Acton TB, et al. (2012) Principles for designing ideal protein structures. Nature 491: 222-227.